

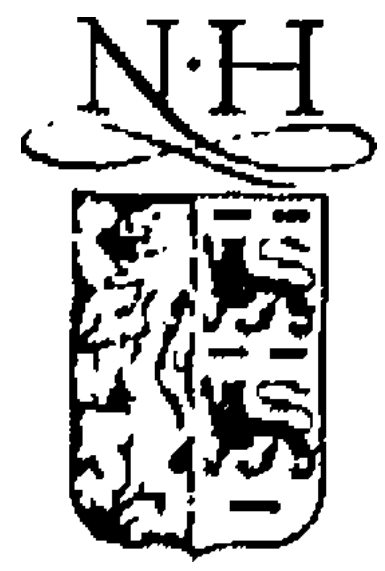
PDF hosted at the Radboud Repository of the Radboud University Nijmegen

The following full text is a publisher's version.

For additional information about this publication click this link.

<http://hdl.handle.net/2066/26840>

Please be advised that this information was generated on 2019-09-19 and may be subject to change.



ELSEVIER

26 May 1994

PHYSICS LETTERS B

Physics Letters B 328 (1994) 223–233

Measurement of inclusive production of neutral hadrons from Z decays

L3 Collaboration

M. Acciarri^y, A. Adam^{aq}, O. Adriani^o, M. Aguilar-Benitez^x, S. Ahlenⁱ, J. Alcaraz^p,
A. Aloisio^{aa}, G. Alverson^j, M.G. Alviggi^{aa}, G. Ambrosi^{af}, Q. An^q, H. Anderhub^{at},
A.L. Andersonⁿ, V.P. Andreev^{aj}, T. Angelescu^k, L. Antonov^{an}, D. Antreasyan^g,
G. Alkhozov^{aj}, P. Arce^x, A. Arefiev^z, T. Azemoon^c, T. Aziz^h, P.V.K.S. Baba^q, P. Bagnaia^{ai},
J.A. Bakken^{ah}, L. Baksay^{ap}, R.C. Ball^c, S. Banerjee^h, K. Banicz^{aq}, J. Bao^e, R. Barillère^p,
L. Barone^{ai}, A. Baschirotto^y, R. Battiston^{af}, A. Bay^r, F. Becattini^o, U. Beckerⁿ, F. Behner^{at},
Gy.L. Bencze^l, J. Berdugo^x, P. Bergesⁿ, B. Bertucci^{af}, B.L. Betev^{an,at}, M. Biasini^{af},
A. Biland^{at}, G.M. Bilei^{af}, R. Bizzarri^{ai}, J.J. Blaising^d, G.J. Bobbink^{p,b}, R. Bock^a, A. Böhm^a,
B. Borgia^{ai}, D. Bourilkov^{at}, M. Bourquin^r, D. Boutigny^p, B. Bouwens^b, E. Brambilla^{aa},
J.G. Branson^{ak}, V. Brigljevic^{af}, I.C. Brock^{ag}, M. Brooks^v, A. Bujak^{aq}, J.D. Burgerⁿ,
W.J. Burger^r, C. Burgos^x, J. Busenitz^{ap}, A. Buytenhuijs^{ac}, A. Bykov^{aj}, X.D. Cai^q,
M. Capellⁿ, M. Caria^{af}, G. Carlino^{aa}, A.M. Cartacci^o, J. Casaus^x, R. Castello^y, N. Cavallo^{aa},
M. Cerrada^x, F. Cesaroni^{ai}, M. Chamizo^x, Y.H. Chang^{av}, U.K. Chaturvedi^q, M. Chemarin^w,
A. Chen^{av}, C. Chen^f, G. Chen^{f,at}, G.M. Chen^f, H.F. Chen^s, H.S. Chen^f, M. Chenⁿ,
G. Chiefari^{aa}, C.Y. Chien^e, M.T. Choi^{ao}, S. Chungⁿ, C. Civinini^o, I. Clareⁿ, R. Clareⁿ,
T.E. Coan^v, H.O. Cohn^{ad}, G. Coignet^d, N. Colino^p, A. Contin^g, S. Costantini^{ai},
F. Cotorobai^k, B. de la Cruz^x, X.T. Cui^q, X.Y. Cui^q, T.S. Daiⁿ, R. D'Alessandro^o,
R. de Asmundis^{aa}, A. Degré^d, K. Deiters^{ar}, E. Dénes^l, P. Denes^{ah}, F. DeNotaristefani^{ai},
D. DiBitonto^{ap}, M. Diemoz^{ai}, H.R. Dimitrov^{an}, C. Dionisi^{ai}, M. Dittmar^{at}, L. Djambazov^{at},
M.T. Dova^{q,3}, E. Drago^{aa}, D. Duchesneau^r, P. Duinker^b, I. Duran^{al}, S. Easo^{af},
H. El Mamouni^w, A. Engler^{ag}, F.J. Epplingⁿ, F.C. Erné^b, P. Extermann^r, R. Fabbretti^{ar},
M. Fabre^{ar}, S. Falciano^{ai}, S.J. Fan^{am}, A. Favara^o, J. Fay^w, M. Felcini^{at}, T. Ferguson^{ag},
D. Fernandez^x, G. Fernandez^x, F. Ferroni^{ai}, H. Fesefeldt^a, E. Fiandrini^{af}, J.H. Field^r,
F. Filthaut^{ac}, P.H. Fisher^e, G. Forconiⁿ, L. Fredj^r, K. Freudenreich^{at}, W. Friebel^{as},
M. Fukushimaⁿ, M. Gailloud^u, Yu. Galaktionov^{z,n}, E. Gallo^o, S.N. Ganguli^h,
P. Garcia-Abia^x, S. Gentile^{ai}, N. Gheordanescu^k, S. Giagu^{ai}, S. Goldfarb^u, Z.F. Gong^s,
E. Gonzalez^x, A. Gougas^e, D. Goujon^r, G. Gratta^{ae}, M. Gruenewald^p, C. Gu^q,
M. Guanzioli^q, J.K. Guo^{am}, V.K. Gupta^{ah}, A. Gurtu^h, H.R. Gustafson^c, L.J. Gutay^{aq},

K. Hangarter^a, A. Hasan^q, D. Hauschildt^b, C.F. He^{am}, J.T. He^f, T. Hebbeker^p, M. Hebert^{ak},
 A. Hervé^p, K. Hilgers^a, H. Hofer^{at}, H. Hoorani^r, S.R. Hou^{av}, G. Hu^q, G.Q. Hu^{am}, B. Ille^w,
 M.M. Ilyas^q, V. Innocente^p, H. Janssen^d, B.N. Jin^f, L.W. Jones^c, I. Josa-Mutuberria^p,
 A. Kasser^u, R.A. Khan^q, Yu. Kamyshkov^{ad}, P. Kapinos^{as}, J.S. Kapustinsky^v, Y. Karyotakis^p,
 M. Kaur^q, S. Khokhar^q, M.N. Kienzle-Focacci^r, J.K. Kim^{ao}, S.C. Kim^{ao}, Y.G. Kim^{ao},
 W.W. Kinnison^v, A. Kirkby^{ae}, D. Kirkby^{ae}, S. Kirsch^{as}, W. Kittel^{ac}, A. Klimentov^{n,z},
 A.C. König^{ac}, E. Koffeman^b, O. Kornadt^a, V. Koutsenko^{n,z}, A. Koulbardi^{aj}, R.W. Kraemer^{ag},
 T. Kramerⁿ, V.R. Krastev^{an,af}, W. Krenz^a, H. Kuijten^{ac}, K.S. Kumar^m, A. Kunin^{n,z},
 P. Ladron de Guevara^x, G. Landi^o, D. Lanske^a, S. Lanzano^{aa}, A. Lebedevⁿ, P. Lebrun^w,
 P. Lecomte^{at}, P. Lecoq^p, P. Le Coultre^{at}, D.M. Lee^v, J.S. Lee^{ao}, K.Y. Lee^{ao}, I. Leedom^j,
 C. Leggett^c, J.M. Le Goff^p, R. Leiste^{as}, M. Lenti^o, E. Leonardi^{ai}, P. Levtchenko^{aj}, C. Li^{s,q},
 H.T. Li^f, P.J. Li^{am}, J.Y. Liao^{am}, W.T. Lin^{av}, Z.Y. Lin^s, F.L. Linde^b, B. Lindemann^a, L. Lista^{aa},
 Y. Liu^q, W. Lohmann^{as}, E. Longo^{ai}, W. Lu^{ae}, Y.S. Lu^f, J.M. Lubbers^p, K. Lübelmeyer^a,
 C. Luci^{ai}, D. Luckey^{g,n}, L. Ludovici^{ai}, L. Luminari^{ai}, W. Luster^{ar}, J.M. Ma^f, W.G. Ma^s,
 M. MacDermott^{at}, L. Malgeri^{ai}, R. Malik^q, A. Malinin^z, C. Maña^x, M. Maolinbay^{at},
 P. Marchesini^{at}, F. Marion^d, A. Marinⁱ, J.P. Martin^w, F. Marzano^{ai}, G.G.G. Massaro^b,
 K. Mazumdar^h, P. McBride^m, T. McMahon^{aq}, D. McNally^{ak}, M. Merk^{ag}, L. Merola^{aa},
 M. Meschini^o, W.J. Metzger^{ac}, Y. Mi^u, A. Mihul^k, G.B. Mills^v, Y. Mir^q, G. Mirabelli^{ai},
 J. Mnich^a, M. Möller^a, B. Monteleoni^o, R. Morand^d, S. Morganti^{ai}, N.E. Moulai^q,
 R. Mount^{ae}, S. Müller^a, E. Nagy^l, M. Napolitano^{aa}, F. Nessi-Tedaldi^{at}, H. Newman^{ae},
 M.A. Niaz^q, A. Nippe^a, H. Nowak^{as}, G. Organtini^{ai}, D. Pandoulas^a, S. Paoletti^{ai},
 P. Paolucci^{aa}, G. Pascale^{ai}, G. Passaleva^{o,af}, S. Patricelli^{aa}, T. Paul^e, M. Pauluzzi^{af}, C. Paus^a,
 F. Pauss^{at}, Y.J. Pei^a, S. Pensotti^y, D. Perret-Gallix^d, J. Perrier^r, A. Pevsner^e, D. Piccolo^{aa},
 M. Pieri^p, J.C. Pinto^{ag}, P.A. Piroué^{ah}, F. Plasil^{ad}, V. Plyaskin^z, M. Pohl^{at}, V. Pojidaev^{z,o},
 H. Postemaⁿ, Z.D. Qi^{am}, J.M. Qian^c, K.N. Qureshi^q, R. Raghavan^h, G. Rahal-Callot^{at},
 P.G. Rancoita^y, M. Rattaggi^y, G. Raven^b, P. Razis^{ab}, K. Read^{ad}, M. Redaelli^y, D. Ren^{at},
 Z. Ren^q, M. Rescigno^{ai}, S. Reucroft^j, A. Ricker^a, S. Riemann^{as}, B.C. Riemers^{aq}, K. Riles^c,
 O. Rind^c, H.A. Rizvi^q, S. Ro^{ao}, A. Robohm^{at}, F.J. Rodriguez^x, B.P. Roe^c, M. Röhner^a,
 S. Röhner^a, L. Romero^x, S. Rosier-Lees^d, R. Rosmalen^{ac}, Ph. Rosselet^u, W. van Rossum^b,
 S. Roth^a, A. Rubbiaⁿ, J.A. Rubio^p, H. Rykaczewski^{at}, M. Sachwitz^{as}, J. Salicio^p,
 J.M. Salicio^x, E. Sanchez^x, G.S. Sanders^v, A. Santocchia^{af}, M.S. Sarakinosⁿ, G. Sartorelli^{g,q},
 M. Sassowsky^a, G. Sauvage^d, C. Schäfer^a, V. Schegelsky^{aj}, D. Schmitz^a, P. Schmitz^a,
 M. Schneegans^d, N. Scholz^{at}, H. Schopper^{au}, D.J. Schotanus^{ac}, S. Shotkinⁿ, H.J. Schreiber^{as},
 J. Shukla^{ag}, R. Schulte^a, K. Schultze^a, J. Schwenke^a, G. Schwering^a, C. Sciacca^{aa}, I. Scott^m,
 R. Sehgal^q, P.G. Seiler^{ar}, J.C. Sens^{p,b}, L. Servoli^{af}, I. Sheer^{ak}, D.Z. Shen^{am}, S. Shevchenko^{ae},
 X.R. Shi^{ae}, E. Shumilov^z, V. Shoutko^z, D. Son^{ao}, A. Sopczak^p, V. Soulimov^{aa}, C. Spartiotis^t,
 T. Spickermann^a, P. Spillantini^o, R. Starosta^a, M. Steuer^{g,n}, D.P. Stickland^{ah}, F. Sticozziⁿ,
 H. Stone^{ah}, K. Strauch^m, K. Sudhakar^h, G. Sultanov^q, L.Z. Sun^{s,q}, G.F. Susinno^r, H. Suter^{at},
 J.D. Swain^q, A.A. Syed^{ac}, X.W. Tang^f, L. Taylor^j, Samuel C.C. Tingⁿ, S.M. Tingⁿ,
 O. Toker^{af}, M. Tonutti^a, S.C. Tonwar^h, J. Tóth^l, A. Tsaregorodtsev^{aj}, G. Tsipolitis^{ag},

C. Tully^{ah}, K.L. Tung^f, T. Tuuva^t, J. Ulbricht^{at}, L. Urbán^l, U. Uwer^a, E. Valente^{ai},
 R.T. Van de Walle^{ac}, I. Vetlitsky^z, G. Viertel^{at}, P. Vikas^q, U. Vikas^q, M. Vivargent^d,
 H. Vogel^{ag}, H. Vogt^{as}, I. Vorobiev^{m,z}, A.A. Vorobyov^{aj}, An.A. Vorobyov^{aj}, L. Vuilleumier^u,
 M. Wadhwa^d, W. Wallraff^a, J.C. Wangⁿ, C.R. Wang^s, X.L. Wang^s, Y.F. Wangⁿ,
 Z.M. Wang^{q,s}, A. Weber^a, J. Weber^{at}, R. Weill^u, J. Wenninger^f, M. Whiteⁿ, C. Willmott^x,
 F. Wittgenstein^p, D. Wright^{ah}, S.X. Wu^q, S. Wynhoff^a, B. Wyslouchⁿ, Y.Y. Xie^{am}, J.G. Xu^f,
 Z.Z. Xu^s, Z.L. Xue^{am}, D.S. Yan^{am}, B.Z. Yang^s, C.G. Yang^f, G. Yang^q, C.H. Ye^q, J.B. Ye^s,
 Q. Ye^q, S.C. Yeh^{av}, Z.W. Yin^{am}, J.M. You^q, N. Yunus^q, M. Yzerman^b, C. Zaccardelli^{ae},
 P. Zemp^{at}, M. Zeng^q, Y. Zeng^a, D.H. Zhang^b, Z.P. Zhang^{s,q}, B. Zhouⁱ, G.J. Zhou^f,
 J.F. Zhou^a, R.Y. Zhu^{ae}, A. Zichichi^{g,p,q}, B.C.C. van der Zwaan^b

^a I. Physikalisches Institut, RWTH, 52056 Aachen, FRG¹

III. Physikalisches Institut, RWTH, 52056 Aachen, FRG¹

^b National Institute for High Energy Physics, NIKHEF, NL-1009 DB Amsterdam, The Netherlands

^c University of Michigan, Ann Arbor, MI 48109, USA

^d Laboratoire d'Annecy-le-Vieux de Physique des Particules, LAPP, IN2P3-CNRS, BP 110, F-74941 Annecy-le-Vieux CEDEX, France

^e Johns Hopkins University, Baltimore, MD 21218, USA

^f Institute of High Energy Physics, IHEP, 100039 Beijing, China

^g INFN-Sezione di Bologna, I-40126 Bologna, Italy

^h Tata Institute of Fundamental Research, Bombay 400 005, India

ⁱ Boston University, Boston, MA 02215, USA

^j Northeastern University, Boston, MA 02115, USA

^k Institute of Atomic Physics and University of Bucharest, R-76900 Bucharest, Romania

^l Central Research Institute for Physics of the Hungarian Academy of Sciences, H-1525 Budapest 114, Hungary²

^m Harvard University, Cambridge, MA 02139, USA

ⁿ Massachusetts Institute of Technology, Cambridge, MA 02139, USA

^o INFN Sezione di Firenze and University of Florence, I-50125 Florence, Italy

^p European Laboratory for Particle Physics, CERN, CH-1211 Geneva 23, Switzerland

^q World Laboratory, FBLJA Project, CH-1211 Geneva 23, Switzerland

^r University of Geneva, CH-1211 Geneva 4, Switzerland

^s Chinese University of Science and Technology, USTC, Hefei, Anhui 230 029, China

^t SEFT, Research Institute for High Energy Physics, P.O. Box 9, SF-00014 Helsinki, Finland

^u University of Lausanne, CH-1015 Lausanne, Switzerland

^v Los Alamos National Laboratory, Los Alamos, NM 87544, USA

^w Institut de Physique Nucléaire de Lyon, IN2P3-CNRS, Université Claude Bernard, F-69622 Villeurbanne Cedex, France

^x Centro de Investigaciones Energeticas, Medioambientales y Tecnológicas, CIEMAT, E-28040 Madrid, Spain

^y INFN-Sezione di Milano, I-20133 Milan, Italy

^z Institute of Theoretical and Experimental Physics, ITEP, Moscow, Russia

^{aa} INFN-Sezione di Napoli and University of Naples, I-80125 Naples, Italy

^{ab} Department of Natural Sciences, University of Cyprus, Nicosia, Cyprus

^{ac} University of Nymegen and NIKHEF, NL-6525 ED Nymegen, The Netherlands

^{ad} Oak Ridge National Laboratory, Oak Ridge, TN 37831, USA

^{ae} California Institute of Technology, Pasadena, CA 91125, USA

^{af} INFN-Sezione di Perugia and Università Degli Studi di Perugia, I-06100 Perugia, Italy

^{ag} Carnegie Mellon University, Pittsburgh, PA 15213, USA

^{ah} Princeton University, Princeton, NJ 08544, USA

^{ai} INFN-Sezione di Roma and University of Rome, "La Sapienza", I-00185 Rome, Italy

^{aj} Nuclear Physics Institute, St. Petersburg, Russia

^{ak} University of California, San Diego, CA 92093, USA

^{al} Dept. de Fisica de Partículas Elementales, Univ. de Santiago, E-15706 Santiago de Compostela, Spain

^{am} Shanghai Institute of Ceramics, SIC, Shanghai, China

^{an} Bulgarian Academy of Sciences, Institute of Mechatronics, BU-1113 Sofia, Bulgaria

^{ao} Center for High Energy Physics, Korea Advanced Inst. of Sciences and Technology, 305-701 Taejon, Republic of Korea

^{ap} University of Alabama, Tuscaloosa, AL 35486, USA^{aq} Purdue University, West Lafayette, IN 47907, USA^{ar} Paul Scherrer Institut, PSI, CH-5232 Villigen, Switzerland^{as} DESY-Institut für Hochenergiephysik, 15738 Zeuthen, FRG^{at} Eidgenössische Technische Hochschule, ETH Zürich, CH-8093 Zürich, Switzerland^{au} University of Hamburg, 22761 Hamburg, FRG^{av} High Energy Physics Group, Taiwan, China

Received 28 March 1994

Editor: K. Winter

Abstract

We present a study of the inclusive production of π^0 , η , K_s^0 and Λ based on 929,000 hadronic Z decays recorded with the L3 detector at LEP. The measured inclusive momentum distributions have been compared with predictions from parton shower models as well as an analytical Quantum Chromodynamics calculation. Comparing to low energy e^+e^- data, we find that QCD describes the energy evolution of the hadron spectrum.

1. Introduction

We report on a measurement of inclusive production of π^0 , η , K_s^0 and Λ at the Z resonance using the L3 detector at LEP. The π^0 and η mesons are detected through their two-photon decay modes as narrow peaks in the $\gamma\gamma$ invariant mass distribution. The K_s^0 and Λ are identified by their decays into two charged particles, $K_s^0 \rightarrow \pi^+\pi^-$ and $\Lambda \rightarrow p\pi^-$, which are selected using the clear separation of the decay point from the e^+e^- vertex.

We compare the measured inclusive momentum spectra with the predictions of two Monte Carlo generators. Both programs implement a parton cascade based on perturbative QCD calculations, while the non-perturbative hadronization phase is described by either string (JETSET 7.3 [1]) or cluster fragmentation (HERWIG 5.4 [2]) models.

We also compare the measured spectra with analytical calculations performed in the framework of the “Modified Leading Log Approximation” (MLLA) of QCD [3], in which single and double leading-log contributions are taken into account and coherence ef-

fects of soft gluons are included [4]. Complemented with the “Local Parton-Hadron Duality” assumption [3,5], where the non-perturbative effects are reduced to normalization constants relating multiplicities at the hadron level to those at the parton level, the calculated MLLA inclusive parton spectra can be directly compared with the measured hadron spectra.

Experimental studies of charged and neutral particles have been performed before at LEP [6,7]. In this paper we update our previous analysis on π^0 [8] and η [9] using much higher statistics data and present new results on K_s^0 and Λ .

2. The L3 detector

The L3 detector is described in detail in Ref. [10]. It consists of a central tracking chamber, a high resolution electromagnetic calorimeter composed of bismuth germanium oxide (BGO) crystals, a ring of plastic scintillation counters, a uranium and brass hadron calorimeter with proportional wire chamber readout, and an accurate muon chamber system. These detectors are installed in a 12 m diameter magnet which provides a uniform field of 0.5 T along the beam direction.

The central tracking chamber (TEC) is a time expansion chamber with high spatial resolution in the plane normal to the beam. A Z-chamber, mounted just outside the TEC, supplements the r/ϕ measurements

¹ Supported by the German Bundesministerium für Forschung und Technologie.

² Supported by the Hungarian OTKA fund under contract number 2970.

³ Also supported by CONICET and Universidad Nacional de La Plata, CC 67, 1900 La Plata, Argentina.

with z-coordinates.

The material preceding the barrel part of the electromagnetic detector amounts to less than 10% of a radiation length. In this region the energy resolution is 5% for photons and electrons of energy around 100 MeV, and is less than 2% for energies above 1 GeV. The angular resolution of electromagnetic clusters is better than 0.5° for energies above 1 GeV.

For this analysis, we use the data collected in the following polar angle ranges: for the central tracking chamber $40^\circ < \theta < 140^\circ$; for the electromagnetic calorimeter $11^\circ < \theta < 169^\circ$; and for the hadron calorimeter $5^\circ < \theta < 175^\circ$.

3. Event selection

Events collected at center of mass energies around $\sqrt{s} = 91.2$ GeV ($88.4 \leq \sqrt{s} \leq 93.7$ GeV) during the 1991 and 1992 LEP running periods are used for this analysis, corresponding to an integrated luminosity of 35 pb^{-1} .

The selection of events of the type $e^+e^- \rightarrow \text{hadrons}$ is based on tracking information and the energy measured in the electromagnetic detector and in the hadron calorimeter. Events are accepted if they have high multiplicity, high and well balanced visible energy [11]. In total, 929,000 events pass the selection cuts.

The Monte Carlo samples consist of 1,000,000 events generated using JETSET 7.3 [1] and of 500,000 events generated using HERWIG 5.4 [2]. The values for the QCD scale and the fragmentation parameters were determined from fits to our data [12]. The generated events are passed through the L3 detector simulation [13], which implements a detailed description of the detector and takes into account the effects of energy loss, multiple scattering, interactions and decays in the detector materials and the beam pipe. These events are processed with the same reconstruction and analysis programs as used for the experimental data.

Applying the same selection of hadronic Z decays to the simulated events as for the data, we find that more than 98% of the hadronic decays from the Z are accepted. The contamination from e^+e^- and $\tau^+\tau^-$ final states and from hadronic production via two-photon processes is estimated to be less than 0.2% and is ignored in the following analysis.

3.1. Photon selection

Photon candidates are recognized as isolated clusters in the electromagnetic calorimeter. The photon energy is calculated from the energy of the cluster by applying a position-dependent leakage correction. Assuming that the photon originates at the e^+e^- interaction point, its direction is determined from the center of gravity of the shower. The photons used in this analysis are required to satisfy the following cuts:

- (1) the candidate is in the barrel region, $|\cos \theta_\gamma| < 0.74$;
- (2) the energy of the candidate is greater than 50 MeV for π^0 selection and greater than 500 MeV for η selection;
- (3) the candidate is separated by at least 50 mrad from any charged particle;
- (4) the lateral shower shape of the candidate is consistent with that of an electromagnetic shower.

Cut (2) is used to reject noise and to reduce the background from hadrons. The background of hadrons is further reduced by cuts (3) and (4), where the reference shower shape of photons is determined from test beam data. The selection efficiency for photons from π^0 decay is about 23% with a purity of about 70%.

3.2. Secondary vertex selection

In order to detect secondary vertices we examine all two-track combinations with opposite charge, searching for intersections in the r/ϕ -plane. Tracks have to be well measured in the central tracking chamber as well as the Z-chamber, with a momentum transverse to the beam axis of more than 150 MeV. Their distance of closest approach (DCA) to the primary e^+e^- vertex must be greater than 1 mm. This primary vertex is determined on a fill-by-fill basis and is assumed to be the origin of K_s^0 and Λ .

We apply further cuts to reject the background created by randomly intersecting tracks from the event vertex. The angle between the transverse flight direction, d_t , and the total transverse momentum of the pair, p_t , must be smaller than 30 mrad. To eliminate combinations of tracks belonging to different jets, the product of p_t and the opening angle of the two tracks measured at the candidate secondary vertex must be less than 1.1 rad·GeV. We further require that the distance d_t between the secondary vertex and the primary

vertex is greater than 10 mm. If the intersection point lies in the volume of the tracking chamber, we require that the pattern of hit wires be consistent with a neutral particle decay. Finally, the probability that the neutral hadron candidate decayed within the distance d_t from the production point must be less than 98.5%.

To complete the kinematical reconstruction of the decay, the polar angles of the particle momenta are redetermined from a fit using the Z-chamber points, constrained by applying longitudinal momentum conservation and a common origin for the charged tracks.

The selection efficiency is obtained by applying the same criteria to Monte Carlo JETSET and HERWIG events. The resulting efficiency and its time dependence are verified using a sample of $Z \rightarrow \mu^+ \mu^-$ events taken in the same running period. The simulated momentum and DCA resolutions have been checked to be the same as in the measured data.

4. Inclusive hadron multiplicities

The $\gamma\gamma$ invariant mass spectrum is measured using photon pairs in which both photons are in the same hemisphere as defined by a plane perpendicular to the event thrust axis in order to reduce the combinatorial background.

The reconstructed invariant mass spectrum of any two photons fulfilling the criteria for π^0 selection is shown in Fig. 1a. The spectrum is fitted using a Gaussian distribution for the signal plus a third order polynomial for the background. The number of π^0 's from the fit is 387225 ± 1087 where the error is statistical only. The fitted mass is compatible with the value from the Particle Data Group (PDG) [14] and the width is 7.6 MeV, compatible with the detector resolution. A mass window of $0.113 < m_{\gamma\gamma} < 0.157$ GeV gives a π^0 selection efficiency of about 4.2% with a purity of 50%.

The η signal is observed in a restricted two-photon mass spectrum as shown in Fig. 1b. To reduce the combinatorial background related to π^0 decays, we exclude all photons entering into a two-photon combination with invariant mass inside the π^0 window. The same fitting method as that for π^0 is applied and gives 7276 ± 152 as the observed number of η mesons. The mass is compatible with the PDG value; the width is 17.8 MeV, again consistent with the detector res-

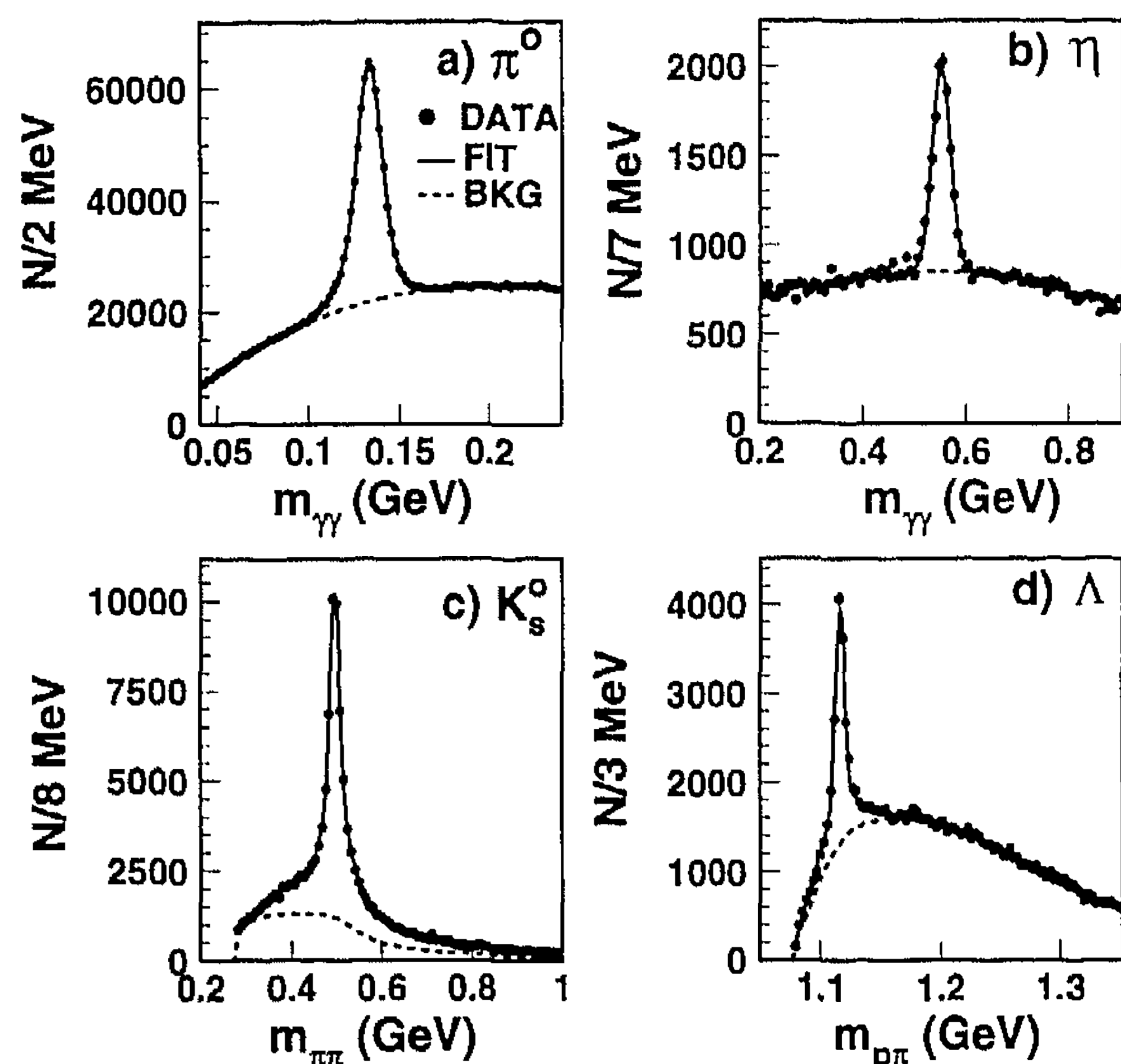


Fig. 1. The measured $\gamma\gamma$, $\pi^+\pi^-$ and $p\pi^-$ ($\bar{p}\pi^+$) invariant mass distribution. The solid lines in the π^0 and η mass plots represent the results of fits to the data using a sum of a Gaussian distribution and a third order polynomial. The dashed lines indicate the fitted background. In the $\pi^+\pi^-$ and $p\pi^-$ ($\bar{p}\pi^+$) mass plots, the solid lines are fits to the data using a sum of two Gaussian distributions and a third order polynomial. The dashed lines indicate the background estimated from the Monte Carlo.

olution. Inside a mass window of $0.500 < m_{\gamma\gamma} < 0.590$ GeV the efficiency to detect an η decay into two photons is 2.1%, with a purity of about 40%.

The selection efficiency for the signal is determined from Monte Carlo as the ratio of the fitted number of π^0 and η to the respective number of generated particles. In this way our results are independent of the Monte Carlo simulation of the background and the width of the signal. Due to the different fragmentation schemes, there is a difference between JETSET and HERWIG in the isolation of photons. This leads to different selection efficiencies and cross sections. As both models otherwise provide a reasonable description of the data [12], we take the average of the multiplicities determined both ways as the result, assigning half the differences to the systematic errors. The resultant multiplicities are shown in Table 1 and compared with the Monte Carlo predictions. The measured multiplicity in the accessible x_p range, where x_p is defined as the ratio of the particle momentum to the beam energy, are quoted. They are also extrapolated to the whole momentum range using the corresponding

Table 1
Measured average multiplicity of neutral hadrons per hadronic Z decay

Hadron	x_p Range	JETSET		HERWIG		Multiplicity
		Meas.	Pred.	Meas.	Pred.	
π^0	$0.003 < x_p < 0.15$	8.92	8.79	7.84	8.95	$8.38 \pm 0.03 \pm 0.67$
	All	9.77	9.63	8.60	9.81	$9.18 \pm 0.03 \pm 0.73$
η	$0.02 < x_p < 0.3$	0.73	0.91	0.67	1.01	$0.70 \pm 0.02 \pm 0.08$
	All	0.95	1.21	0.88	1.31	$0.91 \pm 0.02 \pm 0.11$
K_s^0	$0.003 < x_p < 0.24$	0.92	0.98	0.92	1.00	$0.92 \pm 0.01 \pm 0.07$
	All	1.02	1.08	1.01	1.09	$1.02 \pm 0.01 \pm 0.07$
Λ	$0.009 < x_p < 0.24$	0.32	0.32	0.31	0.40	$0.32 \pm 0.01 \pm 0.04$
	All	0.37	0.37	0.37	0.48	$0.37 \pm 0.01 \pm 0.04$

The measured value using the JETSET and HERWIG Monte Carlo programs for the efficiency calculation are reported separately. The average of the two is listed in the last column as the final result. The first error is statistical and the second systematic.

Monte Carlo predictions.

The first error in the last column of Table 1 is statistical and the second is systematic. Besides the systematic error due to the different fragmentation models, mentioned above, other errors are obtained by varying the photon selection cuts, switching off the requirement on shower isolation from charged particles and changing the π^0 background suppression procedure. An additional error coming from the uncertainty in the detector inefficiency is determined by comparing the π^0 and η rate in different geometrical regions of the detector. A small error due to the limited statistics of Monte Carlo events is also included. These contributions to the systematic errors are added in quadrature.

Within the quoted errors, the agreement of the predicted production rate of π^0 with the observed rate is satisfactory for both models. The observed η multiplicity is lower than either model prediction.

The mass spectrum of K_s^0 candidates (Fig. 1c) is calculated by assigning the π^\pm mass to the pair of tracks which form the secondary vertex. For Λ candidates (Fig. 1d), we assign the proton mass to the higher momentum track and the π^\pm mass to the other one. The probability of a wrong assignment is estimated to be less than 0.6%. Both spectra show a narrow peak with a long non-Gaussian tail, above a smooth background. The fitted masses are in agreement with the PDG values; the widths from a Gaussian fit are 18.8 MeV for K_s^0 and 5.6 MeV for Λ , consistent with the detector resolution. The number of K_s^0 (Λ) is counted bin by bin within a mass window of

400 (70) MeV, subtracting the background estimated with the Monte Carlo. For K_s^0 the background has a shoulder at low masses due to Λ 's with the wrong particle assignment. The background subtraction has been tested by comparing background distributions of data and Monte Carlo in a control sample with all the above mentioned cuts, but where the pair points away from the vertex by more than 50 mrad. The agreement of these two distributions is better than 1%. In total we find 73495 ± 345 K_s^0 's and 13315 ± 200 Λ 's. Inside a mass window of $300 < m_{\pi\pi} < 700$ MeV ($1080 < m_{p\pi} < 1150$ MeV), the detection efficiency for selecting K_s^0 (Λ) is 7.8% (3.7%) with a purity of 63.3% (32.4%).

Using the signal events and the efficiency estimated from the Monte Carlo, we obtain the average multiplicity of the observed hadrons in hadronic Z decays as shown in Table 1. For the K_s^0 we take the average of our results obtained using JETSET and HERWIG and assign half the difference as a systematic error, as described above for the π^0 and η . In the case of Λ , we repeat the same procedure, but exclude from the number of generated particles those coming from decays of long-lived Ξ baryons, which are not usually detectable. Less than 0.2% in our selected Λ sample come from Ξ decays for JETSET, 0.6% for HERWIG. Since HERWIG predicts a Ξ production rate three times larger than that observed [7], whereas JETSET agrees well with the data, we use the latter to estimate the number of Λ 's produced in Ξ decay. We then extrapolate the measured rate in the selected x_p range to

the whole momentum range as we did for π^0 and η .

Besides the systematic error due to the different fragmentation models as mentioned above, other errors are obtained by varying all selection cuts, varying the $K_s^0(\Lambda)$ yield as a background to $\Lambda(K_s^0)$, and changing the signal mass windows. An additional error due to the uncertainty of the TEC momentum resolution and the Z-chamber efficiency is also taken into account. The statistical error on the Monte Carlo events is included. The different contributions to the systematic errors are added in quadrature.

The observed multiplicities for K_s^0 and Λ agree with both model predictions, inside the observed range of x_p as well as extrapolated to the whole spectrum.

5. Momentum spectra of hadrons

To determine the x_p distribution of the reconstructed particles, the above measurement of the hadron production rate is repeated for different x_p intervals. In the final spectra detector resolution effects have been unfolded.

The two Monte Carlo generators differ not only in the total hadron multiplicities and the predicted momentum spectrum, but also in the efficiency to detect a hadron and its momentum dependence. Therefore, Fig. 2a, b, c and d as well as Fig. 3a, b, c and d show the momentum spectra of the hadrons expressed in terms of x_p , compared to the Monte Carlo predictions from JETSET and HERWIG, respectively. In each distribution the efficiency corrections for the data are carried out using the respective generator. The errors shown in the plot correspond to statistical and systematic errors added in quadrature, except that the error due to the model difference in efficiency is not included. The dominant systematic error is that on the overall normalization of the spectra. The energy spectra of π^0 and K_s^0 are rather well predicted in shape by both models. The normalization discrepancy in the Λ spectrum for HERWIG comes essentially from the overestimated Ξ contribution, which entails a much reduced detection efficiency. The η spectrum predicted by either model is too soft.

We also compare the measured spectra with a MLLA QCD calculation [3], following the same method applied in the analysis of π^0 and charged particle spectra in Ref. [8] and η in Ref. [9]. We

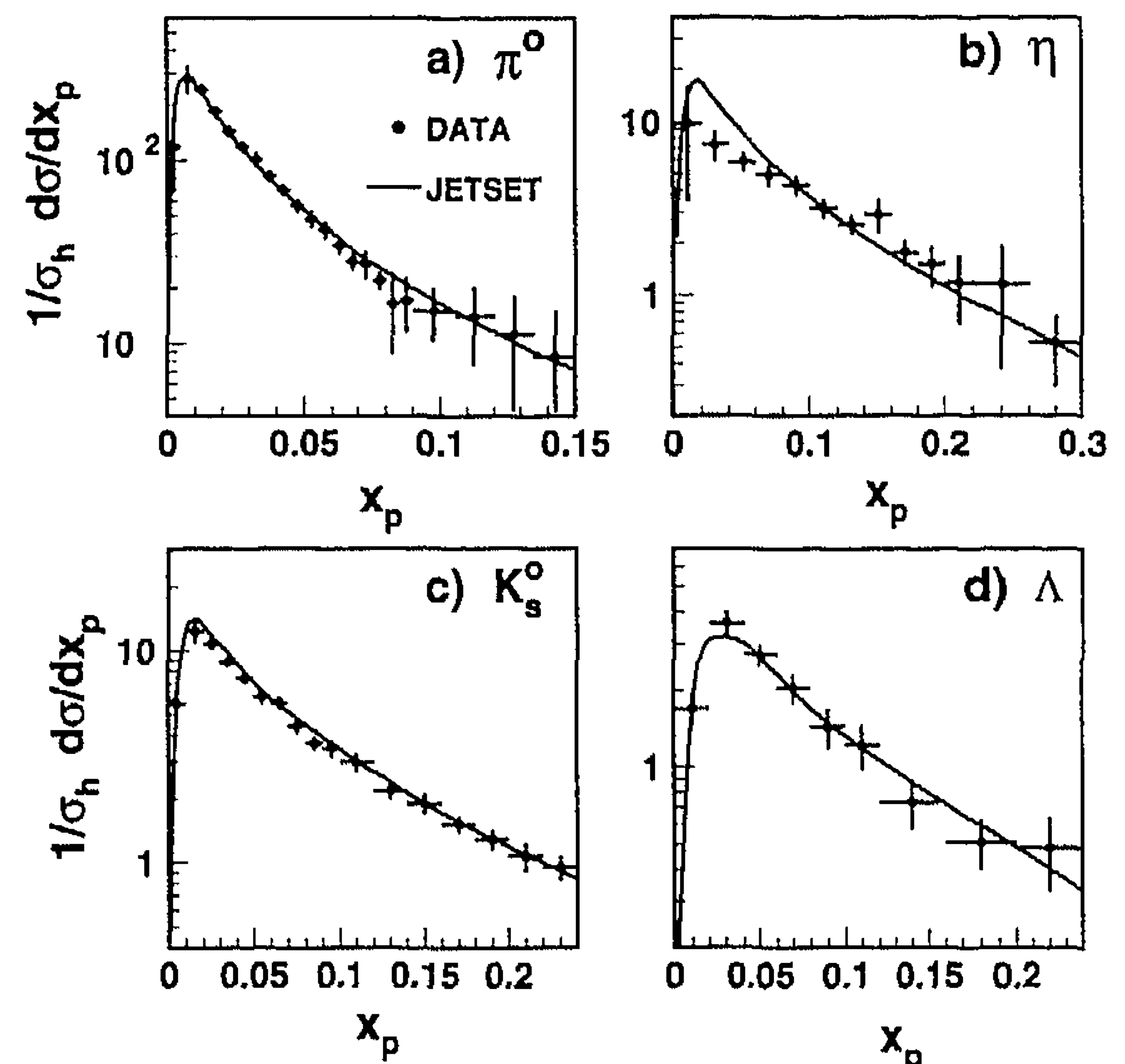


Fig. 2. The x_p spectra at the Z resonance normalized to the total hadronic cross section in comparison with the predictions of the Monte Carlo parton shower generator JETSET. The errors (vertical bars) include statistical and systematic uncertainties added in quadrature as described in the text. The horizontal bars indicate the bin size.

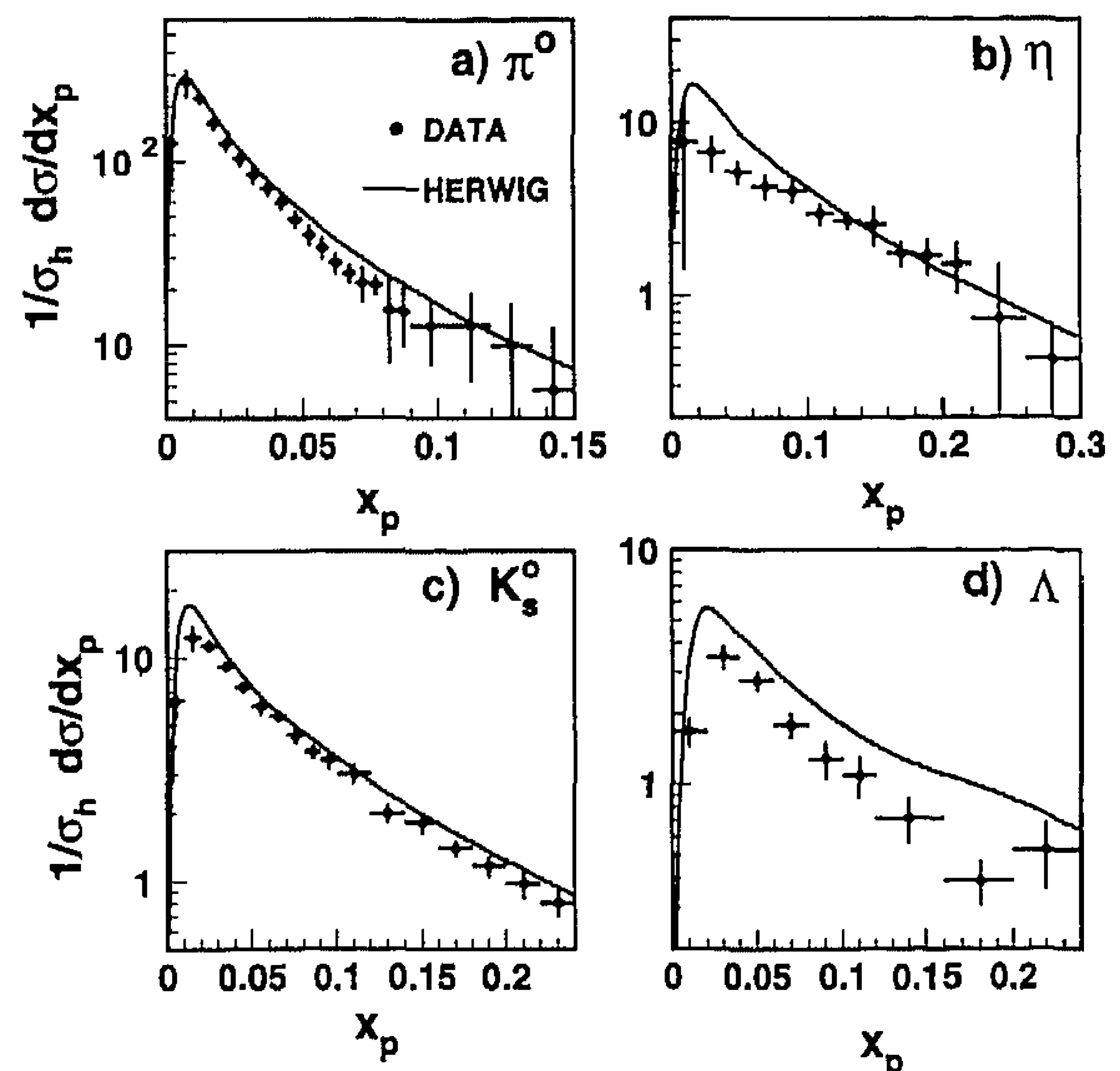


Fig. 3. The x_p spectra at the Z resonance normalized to the total hadronic cross section in comparison with the predictions of the Monte Carlo parton shower generator HERWIG. The errors (vertical bars) include statistical and systematic uncertainties added in quadrature as described in the text. The horizontal bars indicate the bin size.

Table 2
Measured parameters of QCD MLLA corresponding to Eq. (1)

Hadron	N	Λ_{eff} (GeV)	ξ_p^*
π^0	0.492 ± 0.051	0.147 ± 0.030	3.96 ± 0.13
η	0.123 ± 0.016	1.485 ± 0.234	2.52 ± 0.10
K_s^0	0.102 ± 0.005	0.832 ± 0.061	2.89 ± 0.05
Λ	0.041 ± 0.004	0.917 ± 0.178	2.83 ± 0.13

ξ_p^* denotes the position of the maximum corresponding to the value of Λ_{eff} given.

use the MLLA expression for the so-called *limiting spectrum* for hadron type h , which is convenient for numerical integration and can be written in the form:

$$\frac{1}{\sigma_h} \frac{d\sigma}{d\xi_p} = N(\sqrt{s}) \cdot f(\sqrt{s}, \Lambda_{\text{eff}}; \xi_p), \quad (1)$$

where the function f is specified in Ref. [3] and $\xi_p = \ln(1/x_p)$. There are only two free parameters in Eq. (1): an overall normalization factor N , which describes the hadronization and depends on the center of mass energy, \sqrt{s} , and on the particle type, and an effective scale parameter Λ_{eff} (not directly related to $\Lambda_{\overline{\text{MS}}}$). Eq. (1) is valid in the range $1 < \xi_p < \ln(0.5\sqrt{s}/\Lambda_{\text{eff}})$.

Since we do not perform this analysis with respect to a generator, we have to account for differences between the efficiencies predicted by JETSET and HERWIG in the same way as we did in the multiplicity measurement. Therefore, the distributions in ξ_p are evaluated twice, using the JETSET and HERWIG corrections, and the results averaged.

Eq. (1) has two distinct features: the existence of a maximum in the ξ_p distribution; and a prediction for the energy evolution of the position of this maximum. The first feature is illustrated in Fig. 4a, b, c and d, which show our measured differential cross sections $1/\sigma_h \cdot d\sigma/d\xi_p$. We fit Eq. (1) to our data and obtain the results shown in Table 2, where ξ_p^* denotes the position of the maximum corresponding to the measured Λ_{eff} .

For each point, the systematic error dominates over the statistical one. In the fit, we conservatively add statistical and all systematic errors in quadrature for each point even though the overall normalization uncertainty is large. Experimental uncertainties are taken into account by evaluating the results of the fit varying

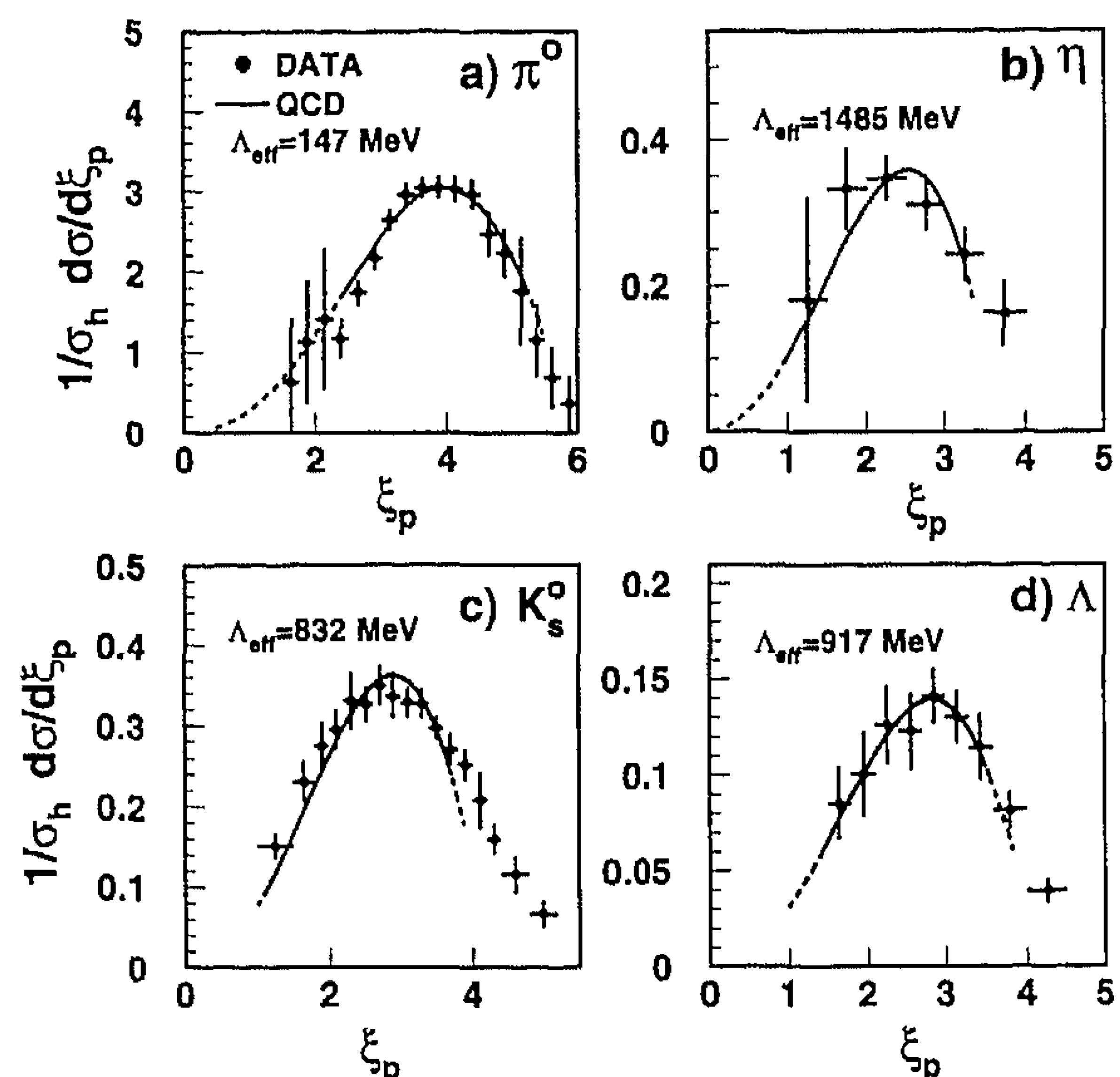


Fig. 4. The inclusive ξ_p spectra normalized to the total hadronic cross section in comparison with analytical QCD calculations (dashed line). The actual fitted region is drawn as a solid line. The data values (dots) are obtained averaging the results derived from efficiency corrections using JETSET and HERWIG. The errors (vertical bars) include statistical and systematic uncertainties added in quadrature as described in the text, except the common normalization uncertainty due to fragmentation. The horizontal bars indicate the bin size.

the parameters and cuts of the analysis. The fragmentation model dependence is then accounted for by averaging the fit results for JETSET and HERWIG and assigning half their difference as the error due to fragmentation. An error due to a variation of the fitted region is also included. All these errors are then added in quadrature and shown in Table 2. The QCD prediction for $\sqrt{s} = 91$ GeV based on the fitted parameters is shown in Fig. 4. The solid lines indicate the actual fitted range in which the predictions are valid; the dashed lines indicate how a pure QCD prediction would extend from this range.

Using our measured Λ_{eff} we can predict ξ_p^* as a function of \sqrt{s} (Fig. 5). Results from other experiments at lower energies [15] are also shown in the plot. The line corresponds to the extrapolation from our high energy result to lower energies. The energy evolution of the peak positions is consistent with the QCD formula, Eq. (1), and our measured Λ_{eff} is valid for different \sqrt{s} . The above measurements are in good

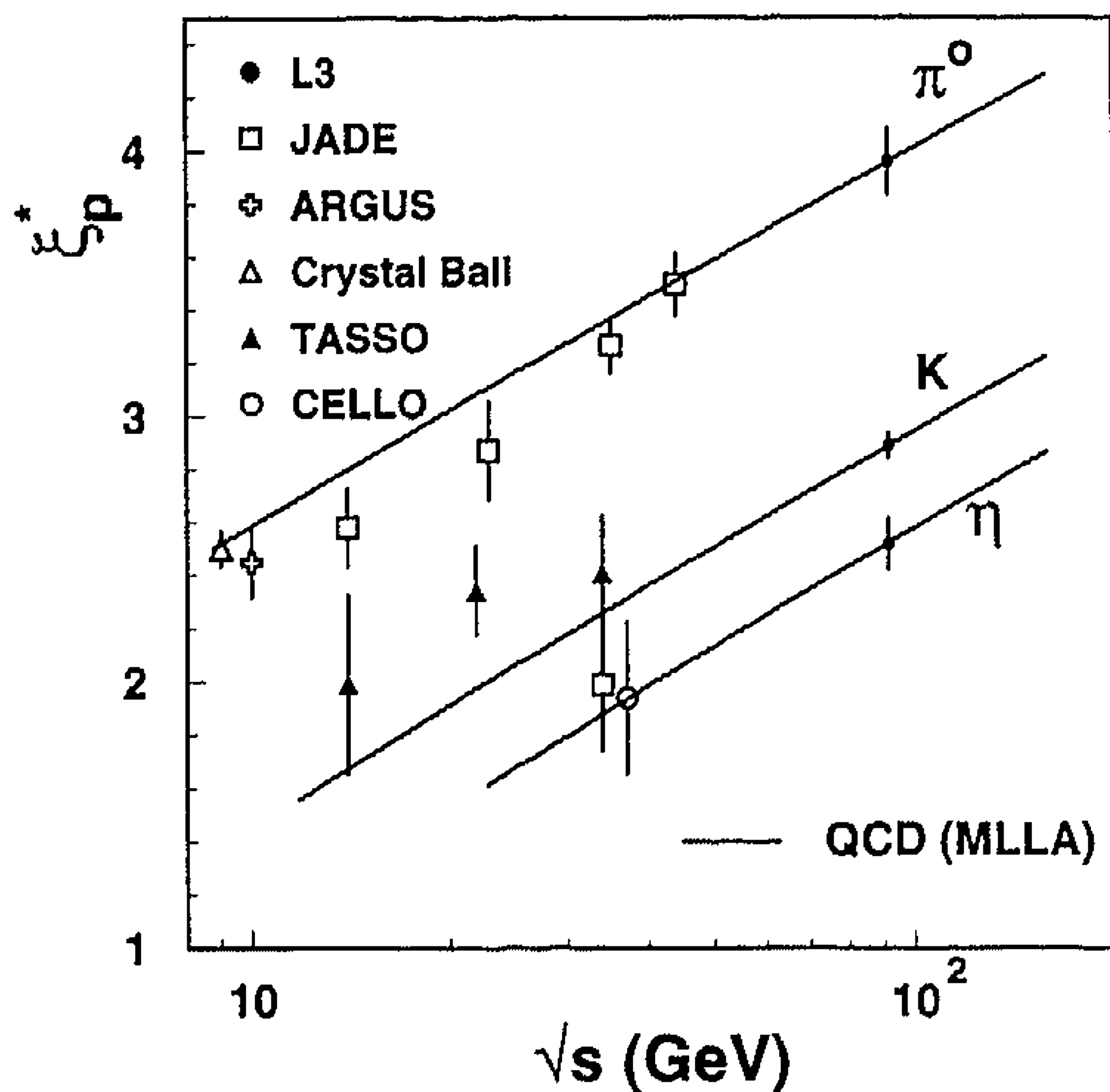


Fig. 5. The energy dependence of the position of the maximum, ξ_p^* , in the ξ_p distributions for π^0 , η and K . The lines represent the QCD MLLA predictions extrapolated from $\sqrt{s} = 91$ GeV. The low energy points are refitted using the same procedure as described in this paper. The results from TASSO are K^\pm while that from L3 is K_s^0 . Different points at the same center of mass energy are shifted horizontally.

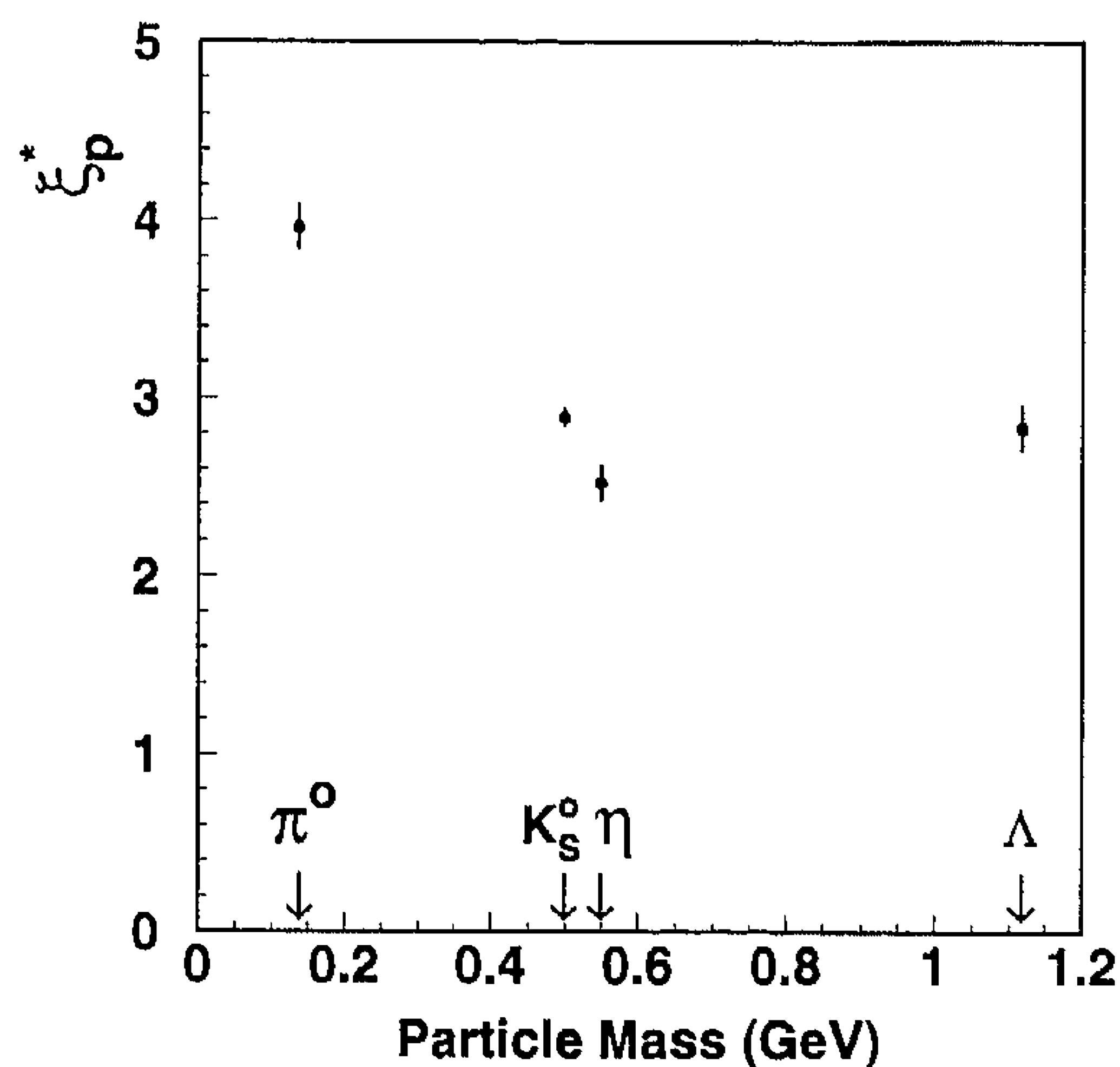


Fig. 6. The position of the maximum, ξ_p^* , in the measured ξ_p distributions for different particles at $\sqrt{s} = 91$ GeV versus particle mass.

agreement with the MLLA calculation⁴.

In Fig. 6 we present ξ_p^* versus particle mass at $\sqrt{s} = 91$ GeV. There is no quantitative prediction for the evolution of ξ_p^* (Λ_{eff}) as a function of particle mass.

⁴ For an alternative approach, see also Ref. [16].

However, it can be seen that most of the particles have similar ξ_p^* values except the π^0 . The neutral pions come mainly from secondary decays and thus have a softer spectrum than hadrons coming directly from fragmentation. Other LEP experiments give similar results [6,7].

6. Summary and conclusions

We have measured the production of the π^0 , η , K_s^0 and Λ from hadronic Z decays. The shape of the measured inclusive momentum distributions of all the hadrons except the η are well reproduced by the Monte Carlo parton shower programs JETSET 7.3 and HERWIG 5.4. For η production the observed spectrum is harder than either prediction. We have also observed that analytical QCD calculations provide a consistent way to describe the shape and the energy evolution of the spectra of hadrons. These measurements significantly improve our previous measurements [8,9].

Acknowledgments

We wish to express our gratitude to the CERN accelerator divisions for the excellent performance of the LEP machine. We acknowledge the effort of all engineers and technicians who have participated in the construction and maintenance of this experiment.

References

- [1] JETSET Monte Carlo Program:
T. Sjöstrand, Comp. Phys. Comm. 39 (1986) 347;
T. Sjöstrand and M. Bengtsson, Comp. Phys. Comm. 43 (1987) 367.
- [2] HERWIG Monte Carlo Program:
G. Marchesini and B. Webber, Nucl. Phys. B 310 (1988) 461;
I.G. Knowles, Nucl. Phys. B 310 (1988) 571;
G. Marchesini et al., Comp. Phys. Comm. 67 (1992) 465.
- [3] Y.L. Dokshitzer and S.I. Troyan, Leningrad Preprint LNPI-922 (1984);
Y.I. Azimov et al., Z. Phys. C 27 (1985) 65; C 31 (1986) 213;
V.A. Khoze, Y.L. Dokshitzer and S.I. Troyan, Lund Preprint LU TP 90-12.
- [4] A.H. Mueller, Phys. Lett. B 104 (1981) 161;
B.I. Ermolaev and V.S. Fadin, JETP Lett. 33 (1981) 285;
A. Bassetto, M. Ciafaloni, G. Marchesini and A.H. Mueller,

- Nucl. Phys. B 207 (1982) 189;
Y.L. Dokshitzer, V.S. Fadin and V.A. Khoze, Phys. Lett. B 115 (1982) 242.
- [5] D. Amati and G. Veneziano, Phys. Lett. B 83 (1979) 87.
- [6] ALEPH Collab., D. Buskulic et al., Phys. Lett. B 292 (1992) 210;
DELPHI Collab., P. Abreu et al., Phys. Lett. B 298 (1993) 236;
DELPHI Collab., P. Abreu et al., Phys. Lett. B 318 (1993) 249;
OPAL Collab., M.Z. Akrawy et al., Phys. Lett. B 247 (1990) 617;
OPAL Collab., G. Alexander et al., Phys. Lett. B 264 (1991) 467;
OPAL Collab., P.D. Acton et al., Phys. Lett. B 305 (1992) 407;
OPAL Collab., P.D. Acton et al., Z. Phys. C 56 (1992) 521.
- [7] DELPHI Collab., P. Abreu et al., Phys. Lett. B 275 (1992) 231;
OPAL Collab., P.D. Acton et al., Phys. Lett. B 291 (1992) 503.
- [8] L3 Collab., B. Adeva et al., Phys. Lett. B 259 (1991) 199.
- [9] L3 Collab., O. Adriani et al., Phys. Lett. B 286 (1992) 403.
- [10] L3 Collab., B. Adeva et al., Nucl. Instr. Meth. A 289 (1990) 35;
L3 Collab., O. Adriani et al., Phys. Rep. 236 (1993) 1.
- [11] L3 Collab., M. Acciarri et al., Measurement of Cross Sections and Leptonic Forward-Backward Asymmetries at the Z pole and Determination of Electroweak Parameters, CERN Preprint PPE/94-45 (March 1994), to be published in Z. Phys.
- [12] L3 Collab., B. Adeva et al., Z. Phys. C 55 (1992) 39.
The parameters of HERWIG have been retuned using the data of heavy flavor decays. The optimum parameters are: CLMAX=3.2, QC DLAM=0.17, VPCUT=0.5, CLPOW=1.45, BILIM=0.35.
- [13] The L3 detector simulation is based on GEANT Version 3.14, November 1990; see R. Brun et al., "GEANT 3", CERN DD/EE/84-1 (Revised), Sept. 1987.
The GHEISHA program (H. Fesefeldt, RWTH Aachen Report PITHA 85/02 (1985)) is used to simulate hadronic interactions.
- [14] Particle Data Group, K. Hikasa et al., Phys. Rev. D 45 (1992) 11.6.
- [15] JADE Collab., D.D. Pitzl et al., Z. Phys. C 46 (1990) 1;
JADE Collab., W. Bartel et al., Z. Phys. C 28 (1985) 343;
CELLO Collab., H.-J. Behrend et al., Z. Phys. C 47 (1990) 1;
ARGUS Collab., H. Albrecht et al., Z. Phys. C 46 (1990) 15;
CRYSTAL BALL Collab., C. Bieler et al., Z. Phys. C 49 (1990) 225;
TASSO Collab., M. Althoff et al., Z. Phys. C 22 (1984) 307;
TASSO Collab., A. Braunschweig et al., Z. Phys. C 42 (1989) 189.
- [16] E.R. Boudinov, P.V. Chliapnikov and V.A. Uvarov, Phys. Lett. B 309 (1993) 210.